Characterization of pre-molten globule state of yeast iso-1-cytochrome c and its deletants at pH 6.0 and 25 °C

ARTICLE *in* INTERNATIONAL JOURNAL OF BIOLOGICAL MACROMOLECULES · NOVEMBER 2014

Impact Factor: 2.86 · DOI: 10.1016/j.ijbiomac.2014.10.053

7 AUTHORS, INCLUDING:

Shah Ubaid-ullah
Central University of Kashmir
7 PUBLICATIONS **26** CITATIONS
SEE PROFILE

Md Imtaiyaz Hassan
Jamia Millia Islamia
108 PUBLICATIONS **956** CITATIONS
SEE PROFILE

Asimul Islam
Jamia Millia Islamia
57 PUBLICATIONS **284** CITATIONS
SEE PROFILE

Faizan Ahmad
Jamia Millia Islamia
219 PUBLICATIONS **2,536** CITATIONS
SEE PROFILE

International Journal of Biological Macromolecules 72 (2015) 1406–1418

Contents lists available at ScienceDirect

International Journal of Biological Macromolecules

journal homepage: www.elsevier.com/locate/ijbiomac

Characterization of pre-molten globule state of yeast iso-1-cytochrome *c* and its deletants at pH 6.0 and 25 °C

Md. Anzarul Haque[a,1], Shah Ubaid-ullah[a,b,1], Sobia Zaidi[a,1], Md. Imtaiyaz Hassan[a], Asimul Islam[a], Janendra K. Batra[b], Faizan Ahmad[a,*]

[a] *Centre for Interdisciplinary Research in Basic Sciences, Jamia Millia Islamia, New Delhi, 110025, India*
[b] *Immunochemistry Lab, National Institute of Immunology, Aruna Asaf Ali Marg, New Delhi, 110067, India*

ARTICLE INFO

Article history:
Received 18 September 2014
Received in revised form 21 October 2014
Accepted 29 October 2014
Available online 4 November 2014

Keywords:
Yeast iso-1-cytochrome *c*
Protein stability
Protein folding
Molten globule
Pre-molten globule

ABSTRACT

To understand the role of five extra N-terminal residues, we prepared wild type (WT) yeast iso-1-cytochrome *c* (y-cyt-*c*) and its deletants by subsequently deleting these residues. Denaturation of all these proteins induced by LiCl was followed by observing changes in molar absorption coefficient at 405 nm ($\Delta\varepsilon_{405}$), the mean residue ellipticity at 222 nm ($[\theta]_{222}$), and the difference mean residue ellipticity at 409 nm ($\Delta[\theta]_{409}$) near physiological pH and temperature (pH 6.0 and 25 °C). It was observed that in each case LiCl induces biphasic transition, N (native) state ↔ X (intermediate) state ↔ D (denatured) state. The intermediate (X) was characterized by the far-UV, near-UV and Soret circular dichroism, ANS (8-anilino-1-naphthalenesulfonic acid) binding and dynamic light scattering measurements. These measurements led us to conclude that X state of each protein has structural characteristics of PMG (pre-molten globule) state. Thermodynamic stability of all proteins was also determined. It was observed that the N-terminal extension stabilizes the native WT protein but it has no effect on the stability of PMG state. Another state was observed for each protein, in the presence of 0.33 M Na_2SO_4 at pH 2.1, which when characterized showed all structural characteristics of MG (molten globule) state.

1. Introduction

Anfinsen's principle established that all the information needed for a protein to attain its unique three-dimensional structure is coded by its sequence [1]. The kinetics and the path through which an unordered polypeptide chain attains this unique ordered conformation still remains one of the tempting problems in the field of protein chemistry. Levinthal [2] pointed out that achieving this native conformation by a random selection from an astronomical number of available conformations would take ages for a protein to fold. However; the physiological time-scale observed for a protein to fold ranges from few milliseconds to seconds. This paradox provided the first indication that attaining the native conformation cannot be a random-search process; instead it must be guided by defined intermediate(s) which will speed up the process and steer the protein to its unique stable confirmation.

Thus, to understand how a protein attains its unique native conformation, the study of intermediates is essentially important. Study of intermediates provides an insight to the mechanism of protein folding, different domains of a protein (if present) and their order of stabilities [3]. Since these intermediates have fluctuating or flexible structure, they are important for biological functions of a protein such as post-translational modifications, membrane translocation or proteasomal degradation [4–7]. These intermediates can also provide new valuable information about the enzyme mechanism and catalysis [8,9]. On the other hand, these transiently formed intermediates can lead to aggregation and amyloid fiber formation because of exposed aggregation prone sticky-surfaces which are otherwise buried in the native conformation [10,11]. Thus, there is an equal tendency for partly folded intermediates to form native structure or to form aggregates [12,13]. All these findings suggest that the study of intermediates is a key to understand protein folding process. Further, the structural characterization of

Abbreviations: Y-cyt-*c*, yeast iso-1-cytochrome *c*; LiCl, lithium chloride; ANS, 8-anilino-1-naphthalenesulfonic acid; PMG, pre-molten globule; MG, molten globule; WT, wild-type; CD, circular dichroism; UV, ultra-violet; DLS, dynamic light scattering.

* Corresponding author. Tel.: +91 11 26321733; fax: +91 11 26983409.
E-mail address: fahmad@jmi.ac.in (F. Ahmad).
[1] These authors contributed equally to this work.

http://dx.doi.org/10.1016/j.ijbiomac.2014.10.053
0141-8130/

these intermediates can provide valuable insights into the mechanism of protein aggregation which is a cause of number of diseases such as Alzheimer's, Parkinson's, Creutzfeldt–Jacob diseases, etc.

Cytochrome *c* (cyt-*c*), a heme containing protein, serves as a good model to study early events and intermediates because of its easy expression and purification, high solubility and stability and relatively single domain structure [14]. The presence of covalently bound prosthetic group, red-colored heme, and presence of single Trp59 provide multiple spectroscopic probes to structurally characterize the intermediates. Different kinetic and equilibrium intermediates in the folding of cyt-*c* have already been studies [15–20]. The kinetics of folding of A-state of cyt-*c* (induced at pH 2 and 0.5 M NaCl) into N (native) state and the kinetics of formation of A state supported the validity of molten globule (MG) state as a model for the D (unfolded) state ↔ N (native) state transition [21,22]. Akiyama et al. [23] used a novel rapid mixing CD technique, time resolved CD and pH jump experiments and proposed a sequential refolding pathway for the acid denatured cyt-*c*. They proposed that initial hydrophobic collapse precedes much of the helix formation in refolding of cyt-*c*, and a compact unfolded state exists on the unfolding pathway. They also found the presence of two on-pathway intermediates (U ↔ I ↔ II ↔ N) at pH 4.5 and 22 °C. Intermediate I possess ~23% of the α-helical content while intermediate II has ~70%, α-helical content. While intermediate I resembled closely to denatured state, the description of intermediate II was consistent with the definition of the molten globule states [24,25]. Intermediate I which lies between denatured and MG states has been related to pre-molten globule state (PMG) described in some other studies [26–28].

In an attempt to gain insight into the nature of different folding-intermediates of cyt-*c*, we have been carrying out equilibrium denaturation studies of mammalian heart cyts-*c* from horse, cow and goat by weak salt denaturants (LiCl, $LiClO_4$, and $CaCl_2$) near physiological pH and temperature [29–32]. We have shown the existence of two thermodynamically stable intermediates, namely MG and PMG states on the folding/unfolding pathway of these proteins. Though lot of literature is available on MG states, but not much progress has been made to study equilibrium PMG occurring during the reversible folding/unfolding process at or near neutral pH.

The wild type (WT) yeast iso-1-cyt-*c* (y-cyt-*c*) which evolved earlier than the mammalian cyts-c, has five extra N-terminal residues [33]. We have been trying to understand questions: "Is the N-terminal extension required for the stability and/or proper folding?" The answer to the first part of the question has already been provided elsewhere [34]. To answer the other part of the question, we cloned, expressed and purified the WT y-cyt-*c* and its deletants lacking the N-terminal residues as described earlier [34]. To find the effect of the extra five N-terminal residues on the folding of y-cyt-*c*, we performed LiCl-induced denaturations of WT and its each deletant. We observed that LiCl induces a biphasic transition, N ↔ X ↔ D at pH 6.0 and 25 °C. The intermediate state (X) when characterized by the far-UV, near-UV and Soret CD, ANS (8-anilino-1-naphthalenesulfonic acid) binding and DLS (dynamic light scattering) measurements, shows all the common structural characteristics of PMG state [27,35,36]. Characteristics of the PMG state are that it (a) retains about 50% native secondary structure, (b) looses all the native tertiary structure, (c) is more compact than unfolded state (approximately 3–4 times that of the native state in terms of hydrodynamic volume), and (d) binds ANS approximately 4–5 times more weakly than MG state. LiCl-induced transitions of WT and deletants were also analyzed for Gibbs free energy changes associated with the transitions, N ↔ X ↔ D. We report that the N-terminal extension contributes to the stability of the native WT protein but it has no effect on the PMG state.

2. Experimental procedures

2.1. Materials

Lithium chloride, sodium salt of cacodylic acid and ANS were procured from Sigma Chemical Co. (USA). Na_2SO_4 was obtained from SD Fine Chemicals, Mumbai (India). Potassium ferricyanide was purchased from Loba Chemical Company. All chemicals and reagents used were analytical-grade reagents.

2.2. Protein expression and purification

Plasmid pBTR1^{SU} harboring the *CYC1* gene that codes for WT y-cyt-*c* and its N-terminal deletants and *CYC3* gene that codes for heme lyase essential for the covalent attachment of the heme to the apo-protein, was used for protein expression. The complete procedure for making deletants, their expression and purification has already been reported [34]. Deletants lacking extra N-terminal residues are denoted by Δ(−5/−5), Δ(−5/−4), Δ(−5/−3), Δ(−5/−2), and Δ(−5/−1) where Δ denotes the deletion and the numbers refer to the residues deleted, e.g., Δ(−5/−1) denotes the deletion of residues numbered from −5 to −1 (i.e., TEFKA), while Δ(−5/−2) denotes the deletion of resides numbered from −5 to −2 (i.e., TEFK) and so on [37]. In WT protein as well as deletants, Cys102 is replaced by Ser (Cys102Ser) to prevent intermolecular disulfide bond formation during denaturation studies [38,39].

2.3. Preparation of protein solutions

Protein solutions were oxidized by adding 0.1% potassium ferricyanide as described earlier [40]. Concentration of protein solutions were determined experimentally using molar absorption coefficient (ε) of 106,100 M^{-1} cm^{-1} at 410 nm [41]. Native protein samples were prepared in 30 mM cacodylate buffer containing 0.1 M NaCl at pH 6.0. A-state was induced by 0.33 M Na_2SO_4 at pH 2.1 [42,43]. For determination of ANS concentration, molar absorption coefficient (ε) of 5000 M^{-1} cm^{-1} at 530 nm was used [44]. Stock solution of LiCl was made in 30 mM cacodylate buffer containing 0.1 M NaCl, and the concentration of the denaturant solution was determined from the value of difference between the refractive indices of the denaturant and the buffer solution using Abbe refractrometer at room temperature [45].

2.4. Absorption measurements

The absorption spectrum of each protein was measured in Shimadzu-1601 UV/vis spectrophotometer having water jacketed cell holder. The temperature of the cell holder was maintained at 25 ± 0.1 °C by circulating water from an external thermostated water bath. Baselines corrections were done with the buffer in question. Spectra were recorded in the wavelength range 800–600 nm. Protein concentration of 80–90 μM was used for absorption measurements. Protein concentration used for LiCl-induced denaturation at 405 nm was in the range 5–7 μM.

2.5. Circular dichroism (CD) measurements

Circular dichroism (CD) spectra and isothermal denaturation of each protein induced by LiCl was measured by CD spectropolarimeter (Jasco-715) equipped with a Peltier-type temperature controller (PTC-348) interfaced with a personal computer. Protein concentration of 14–18 μM was used for CD measurements and 0.1 cm path length cell was used for the far-UV (250–200 nm) and 1.0 cm cell was used for the near-UV (300–270 nm) and Soret

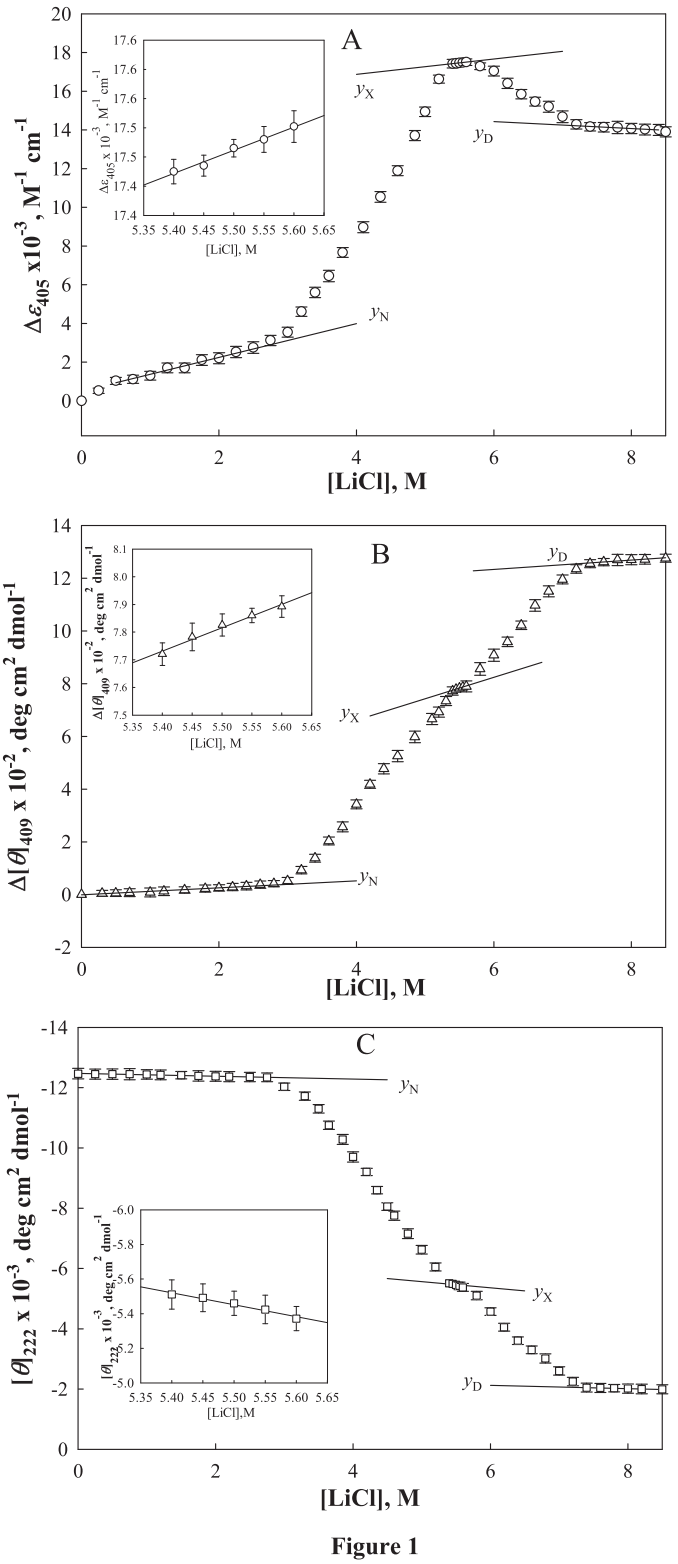

Fig. 1. LiCl-induced denaturation curves of WT y-cyt-*c* at pH 6.0 and 25 °C monitored by change in (A) $\Delta\varepsilon_{405}$, (B) $\Delta[\theta]_{409}$ and (C) $[\theta]_{222}$. The insets show the dependence of y_X, the optical properties of the thermodynamically stable intermediate on [LiCl]. The observed dependencies of $\Delta\varepsilon_{405}$ (M^{-1} cm^{-1}) of N, X and D states of the protein on [LiCl] are described by the relations: $y_N = 916(\pm73)[LiCl] + 437(\pm35)$; $y_X = 412(\pm41)[LiCl] + 15{,}172(\pm283)$; $y_D = -177(\pm56)[LiCl] + 15{,}636(\pm246)$. The observed dependencies of $\Delta[\theta]_{409}$ (deg cm^2 $dmol^{-1}$) of N, X and D states of the protein on [LiCl] are described by the relations: $y_N = 15(\pm2)[LiCl] - 3.7(\pm0.3)$; $y_X = 84(\pm17)[LiCl] - 317(\pm32)$; $y_D = 17(\pm2)[LiCl] - 1127(\pm81)$. The observed dependencies of $[\theta]_{222}$ (deg cm^2 $dmol^{-1}$) of N, X and D states of the protein on [LiCl] are described by the relations: $y_N = 47(\pm11)[LiCl] - 12475(\pm161)$; $y_X = 204(\pm25)[LiCl] - 6587(\pm127)$; $y_D = 56(\pm7)[LiCl] - 2376(\pm107)$. Values in parentheses represent uncertainties from the mean of three or more independent measurements.

(450–370 nm) CD spectral measurements. Each spectrum was corrected for contribution of the blank solution. CD instrument was routinely calibrated with D-10-camphorsulfonic acid. To improve the signal-to-noise ratio, at least five accumulations were made for each scan. CD data were converted to concentration-independent parameter, the mean residue ellipticity $[\theta]$ (deg cm^2 $dmol^{-1}$), using the relation,

$$[\theta]_\lambda = \frac{M_o\theta_\lambda}{10lc} \quad (1)$$

where θ_λ is the observed ellipticity in millidegrees at wavelength λ, M_o is the mean residue weight of the protein, c is the protein concentration in mg ml^{-1}, and l is the path length of the cell in centimeters.

2.6. Fluorescence measurements

Measurements of fluorescence spectra were carried out in Jasco spectroflourimeter (Model FP-6200) in a 3 mm quartz cell at 25 ± 0.1 °C with both excitation and emission slits set at 5 nm band width. The temperature of the cell was maintained by circulating water from an external thermostated water bath. For ANS binding studies, protein samples were incubated with 16-fold molar excess of ANS for 2 h at 25 °C in dark. For these studies, excitation wavelength was set at 360 nm and emission spectra were recorded in the range, 400–600 nm. The protein concentration used was 7–9 μM.

2.7. Dynamic light scattering measurements

To determine hydrodynamic radii of proteins in different solvent conditions, dynamic light scattering (DLS) measurements were carried out in RiNA Laser Spectroscatter (Model-201) at 25 ± 0.1 °C. Samples were filtered through 0.22 μM Millipore syringe filters. Protein concentration of 2.5 mg ml^{-1} was used for the measurements. All measurements were carried out at a fixed angle of 90° using an incident beam of 689 nm. The data were analyzed using PMgr version 3.01 software provided by the manufacturer. For each sample, 10 measurements were made with an acquisition time of 20 s.

3. Results

3.1. LiCl-induced denaturation

LiCl-induced denaturations of WT and its deletants were followed by monitoring the change in $\Delta\varepsilon_{405}$ (difference in ε values in the presence and absence of the denaturant at 405 nm), $[\theta]_{222}$ (mean residue ellipticity at 222 nm), and $\Delta[\theta]_{409}$ (difference in $[\theta]$ values in the presence and absence of the denaturant at 409 nm). It was observed that LiCl induces biphasic transition, N (native) state ↔ X (intermediate) state ↔ D (denatured) state. It should be noted that the WT protein and all its deletants in the native buffer (30 mM cacodylate/cacodylic acid containing 0.1 M NaCl, pH 6.0) will be referred as the native protein. Figs. 1, 2 and S1–S4 show LiCl-induced biphasic denaturation curves of WT, Δ(−5/−4), Δ(−5/−1), Δ(−5/−2), Δ(−5/−3) and Δ(−5/−5) proteins, respectively. It is seen in these figures that the pretransition (y_N) and posttransition (y_D) baselines are well-defined, and the intermediate X, exists in a narrow [LiCl], the molar LiCl concentration, range. To determine the dependence of the optical property of X state (y_X) accurately, we measured it at small concentration intervals of LiCl (see insets

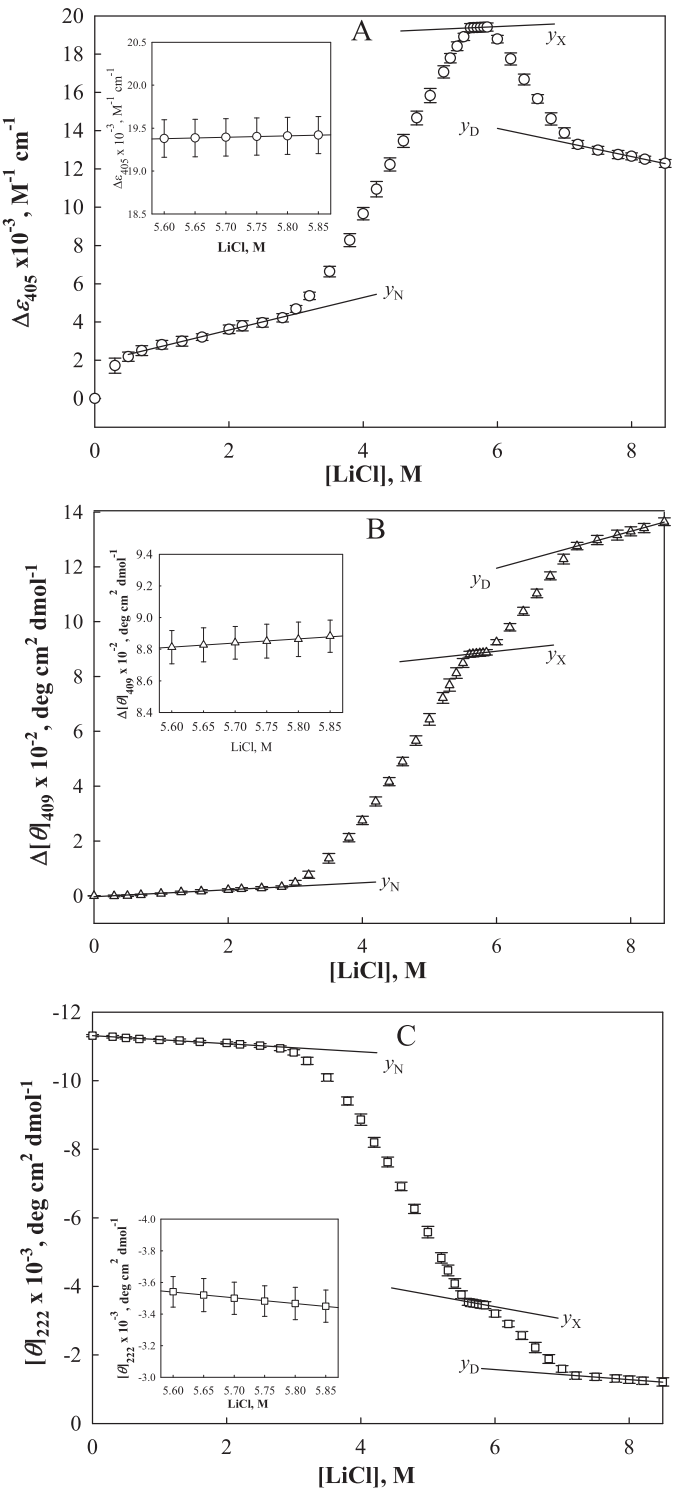

Fig. 2. LiCl-induced denaturation curves of Δ(−5/−4) y-cyt-*c* at pH 6.0 and 25 °C monitored by change in (A) $\Delta\varepsilon_{405}$, (B) $\Delta[\theta]_{409}$ and (C) $[\theta]_{222}$. The insets show the dependence of y_X, the optical properties of the thermodynamically stable intermediate on [LiCl]. The observed dependencies of $\Delta\varepsilon_{405}$ ($M^{-1}\,cm^{-1}$) of N, X and D states of the protein on [LiCl] are described by the relations: $y_N = 851(\pm89)[LiCl] + 1876(\pm142)$; $y_X = 159(\pm30)[LiCl] + 18{,}487(\pm217)$; $y_D = -39(\pm85)[LiCl] + 18{,}560(\pm191)$. The observed dependencies of $\Delta[\theta]_{409}$ (deg cm^2 dmol^{-1}) of N, X and D states of the protein on [LiCl] are described by the relations: $y_N = 13(\pm2)[LiCl] - 3.6(\pm0.4)$; $y_X = 26(\pm4)[LiCl] - 733(\pm41)$; $y_D = 67(\pm7)[LiCl] - 791(\pm53)$. The observed dependencies of $[\theta]_{222}$ (deg cm^2 dmol^{-1}) of N, X and D states of the protein on [LiCl] are described by the relations: $y_N = 117(\pm21)[LiCl] - 11{,}313(\pm185)$; $y_X = 356(\pm40)[LiCl] - 5540(\pm121)$; $y_D = 148(\pm18)[LiCl] - 2462(\pm135)$. Values in parentheses have the same meaning as in Fig. 1.

in Figs. 1, 2 and S1–S4). It should be noted that LiCl-induced denaturation was found to be reversible.

Panel A of Figs. 1, 2 and S1–S4 shows LiCl-induced denaturation curves of WT protein and its deletants monitored by observing changes in $\Delta\varepsilon_{405}$ (a sensitive probe to monitor oxidation state of Fe, heme ligand coordination and heme environment [46,47]) as a function of [LiCl]. For WT protein and each deletant the linear dependencies of y_N, y_X and y_D on [LiCl] were determined and relations describing these dependencies are given in legends of these figures.

Assuming that the process N ↔ X, designated as transition I, follows a two-state mechanism, results shown in panel A of Figs. 1, 2 and S1–S4, were used to calculate f_I (fraction of the molecules in X state) and ΔG_I (Gibbs free energy change associated with transition I) using relations,

$$f_I = \frac{(y - y_N)}{(y_X - y_N)} \tag{2}$$

$$\Delta G_I = -RT \ln\left[\frac{(y - y_N)}{(y_X - y)}\right] \tag{3}$$

where R is the universal gas constant, T is temperature in Kelvin, y is the observed optical property of the protein, and y_N and y_X respectively are optical properties of protein molecules in N and X states at the same [LiCl] at which y has been measured. All values of f_I and values of ΔG_I ($-1.30 \le \Delta G_I$ (kcal mol^{-1}) ≤ 1.30) are plotted as a function of [LiCl] in Figs. 3, S5 and S6. It is seen in these figures that the plot of ΔG_I versus [LiCl] is linear. A linear least-squares analysis was used to obtain values for ΔG_I^0 (value of ΔG_I at 0 M LiCl) and m_I, the slope ($\delta\Delta G_I/\delta$[LiCl]), according to the relation [48],

$$\Delta G_I = \Delta G_I^0 - m_I[LiCl] \tag{4}$$

Values of ΔG_I^0, m_I and C_{mI}, the mid-point of transition I ($C_{mI} = \Delta G_I^0/m_I$) for all proteins are given in Table S1.

Assuming that the process X ↔ D, designated as transition II, also follows a two-state mechanism, we determined values of f_{II} (fraction of molecules in the D state) and ΔG_{II} (Gibbs free energy change associated with transition II) using relations,

$$f_{II} = \frac{(y - y_X)}{(y_D - y_X)} \tag{5}$$

$$\Delta G_{II} = -RT \ln\left[\frac{(y - y_X)}{(y_D - y)}\right] \tag{6}$$

where y is the observed optical property of the protein, and y_X and y_D respectively are optical properties of protein molecules in X and D states at the same [LiCl] at which y has been measured. All values of f_{II} and values of ΔG_{II} ($-1.30 \le \Delta G_I$ (kcal mol^{-1}) ≤ 1.30) are plotted as a function of [LiCl] in Figs. 3, S5 and S6. It is seen in these figures that the plot of ΔG_{II} versus [LiCl] is linear. A linear least-squares analysis was used to obtain values of ΔG_{II}^0 (value of ΔG_{II} at 0 M LiCl), and m_{II}, the slope ($\delta\Delta G_{II}/\delta$[LiCl]), with the help of the relation,

$$\Delta G_{II} = \Delta G_{II}^0 - m_{II}[LiCl] \tag{7}$$

For each protein value of C_{mII}, the mid-point of transition II, was determined from the measured values of ΔG_{II}^0 and m_{II} (i.e., $C_{mII} = \Delta G_{II}^0/m_{II}$). Table S1 shows values of ΔG_{II}^X, C_{mII} and m_{II} of all proteins. It should be noted that ΔG_{II}^X is the value of ΔG_{II} in the presence of LiCl at which X state of a protein exists.

LiCl-induced transition curves were also measured by monitoring changes in $\Delta[\theta]_{409}$ (a probe to monitor heme pocket integrity [49–51]). These curves are shown in panel B of Figs. 1, 2 and S1–S4. Relations describing the dependencies of y_N, y_X and y_D of all proteins on [LiCl] are given in legends of these figures.

Assuming that each transition follows a two-state mechanism, we determined values of f_I, ΔG_I^0, C_{mI}, m_I, f_{II}, ΔG_{II}^X, C_{mII}, m_{II} using

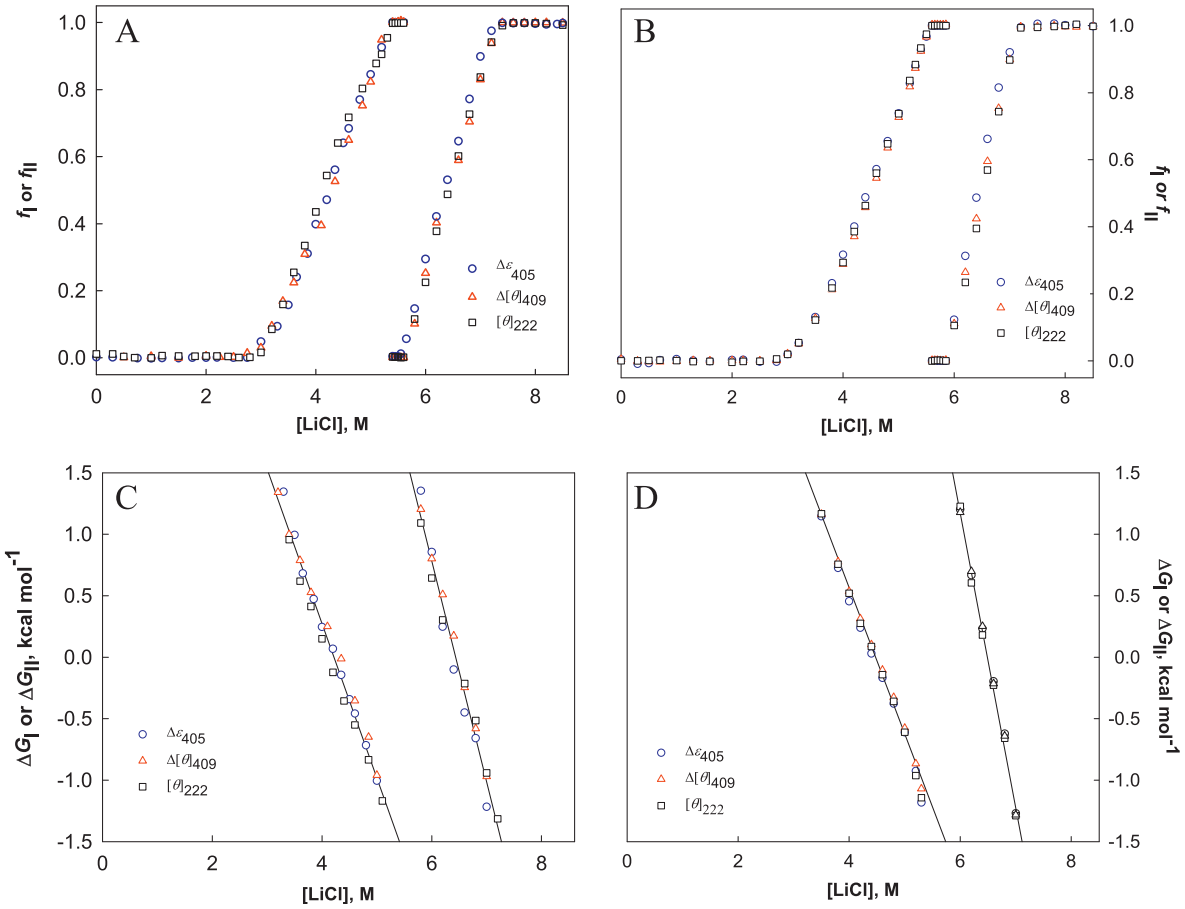

Fig. 3. Plots of f_I and f_{II} of (A) WT y-cyt-*c* and (B) Δ(−5/−4) deletant as a function of [LiCl] and ΔG_I and ΔG_{II} versus [LiCl] for (C) WT and (D) Δ(−5/−4) deletant.

Equations ((2)–(7)). Values of ΔG_I^0, C_{mI}, m_I, ΔG_{II}^X, C_{mII}, m_{II} of WT protein and all deletants are given in Table S1.

Panel C in Figs. 1, 2 and S1–S4 shows LiCl-induced transition curves obtained by monitoring changes in $[\theta]_{222}$ (probe to monitor changes in secondary structure [52,53]) for the WT protein and its deletants. Relations describing the linear dependencies of y_N, y_X and y_D of all proteins on [LiCl] are given in legends of Figs. 1, 2 and S1–S4.

Assuming that each transition follows a two-state mechanism, we determined values of f_I, ΔG_I^0, C_{mI}, m_I, f_{II}, ΔG_{II}^X, C_{mII}, m_{II} using Equations ((2)–(7)). Values of ΔG_I^0, C_{mI}, m_I, ΔG_{II}^X, C_{mII}, m_{II} of WT protein and deletants are given in Table S1.

3.2. Structural characterization of X state

Figs. 4–7 show the far-UV, near-UV and Soret CD spectra and absorption spectra of WT protein and its deletants, respectively. In each figure, curves 1 and 3–5 represent the native state, LiCl-induced X state, LiCl-induced D state and urea-induced D state at pH 6.0 and 25 °C, respectively.

Fig. 8 shows the ANS fluorescence spectra in the presence of WT protein and its deletants in the native state (curve 1), LiCl-induced X state (curve 3), LiCl-induced D state (curve 4) at pH 6.0 and 25 °C.

Hydrodynamic radii of WT protein and its deletants in different solvent conditions were determined by DLS measurements at 25 °C. Values of R_h, the hydrodynamic radius, thus obtained were used to calculate the values of hydrodynamic volume $(4\pi R_h^3/3)$ which are given in Table 1.

3.3. Structural characteristics of A state

It has been shown earlier that addition of 0.33 M Na_2SO_4 to the acid denatured WT y-cyt-*c* (pH 2.1) gives a compact intermediate state, termed as A state which resembles MG [42,43]. To see whether deletants of WT y-cyt-*c* are also transformed into MG state under identical solvent conditions, we denatured these proteins by bringing the pH to 2.1, and to it we added 0.33 M Na_2SO_4. The resultant state of each deletant was characterized by the far-UV, near-UV and Soret CD, ANS binding fluorescence and DLS measurements at pH 2.1 and 25 °C. All the structural characteristics of A state are given in Table 1 (see curve 2 in Figs. 4–8).

4. Discussion

The preceding section presents results on the characterization of the thermodynamically stable intermediate, X, occurring on the LiCl-induced reversible denaturation of WT y-cyt-*c* and its deletants at pH 6.0 and 25 °C. Results on the characterization of A state of each protein, induced by 0.33 M Na_2SO_4 at pH 2.1, are also presented in the previous section. Now these observations are discussed to show that intermediate X and A state have all structural characteristics of PMG and MG, respectively.

4.1. Pre-molten globule state

Intermediate state, X, obtained during LiCl-induced denaturation at pH 6.0 and 25 °C, was structurally characterized with various spectroscopic techniques. We measured the far-UV CD spectra of all proteins in the native state (curve 1), X state (curve 3)

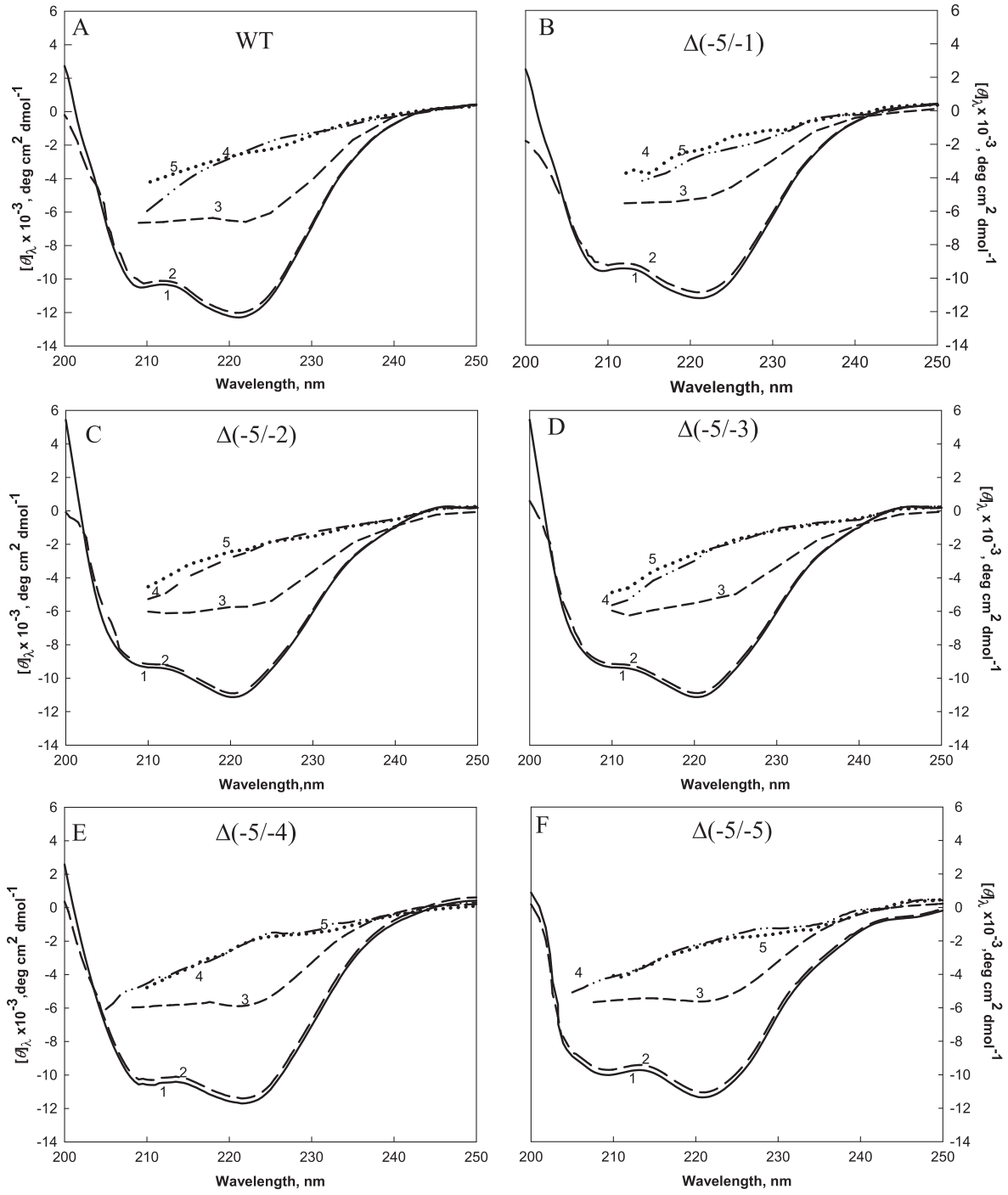

Fig. 4. The far-UV CD spectra of various states of WT y-cyt-*c* and its deletants at pH 6.0 and 25 °C. Native protein (curve 1); A state (curve 2); LiCl-induced X state (curve 3); LiCl-induced D state (curve 4); and urea-induced D state (curve 5). The curve numbers have the same meaning in all panels. Acid denatured, A state (MG) was induced at pH 2.1 and 0.33 M Na_2SO_4 (see text).

and D states induced by LiCl (curve 4) and urea (curve 5) at pH 6.0 and 25 °C (see Fig. 4). The far-UV CD spectrum that we obtained for the WT native protein is in good agreement with the one previously reported earlier [54]. It is seen in Fig. 4 that for each protein, the spectrum of X state (curve 3) lies between spectra of N (curve 1) and D (curves 4 and 5) states. If we take $[\theta]_{222}$ as a probe to measure change in secondary structure, then secondary structure retained in X state of all six proteins lies in the range 40–45% of that of the native state. This observation implies that X state possesses one of the structural characteristics of PMG state, namely, retention of about 50% of secondary structure of the native protein [35,36].

To ascertain whether X state has other PMG like characteristics, we measured the near-UV CD spectra (300–270 nm) of the WT protein and its deletants in the native state (curve 1), X state (curve 3) and D states induced by LiCl (curve 4) and urea (curve 5) at pH 6.0 and 25 °C (see Fig. 5). The near-UV CD arises due to tight packing of side chains of aromatic amino acid residues (one Trp, four Phe and five Tyr residues) and two thioether bonds present in the native cyt-*c* [55]. The presence of two characteristic negative peaks in the region 282–289 nm, arising from interaction of Trp59 with one heme propionate, is a signature of the natively folded cyts-*c* [33,55]. The near-UV CD spectrum obtained for the native WT protein is in

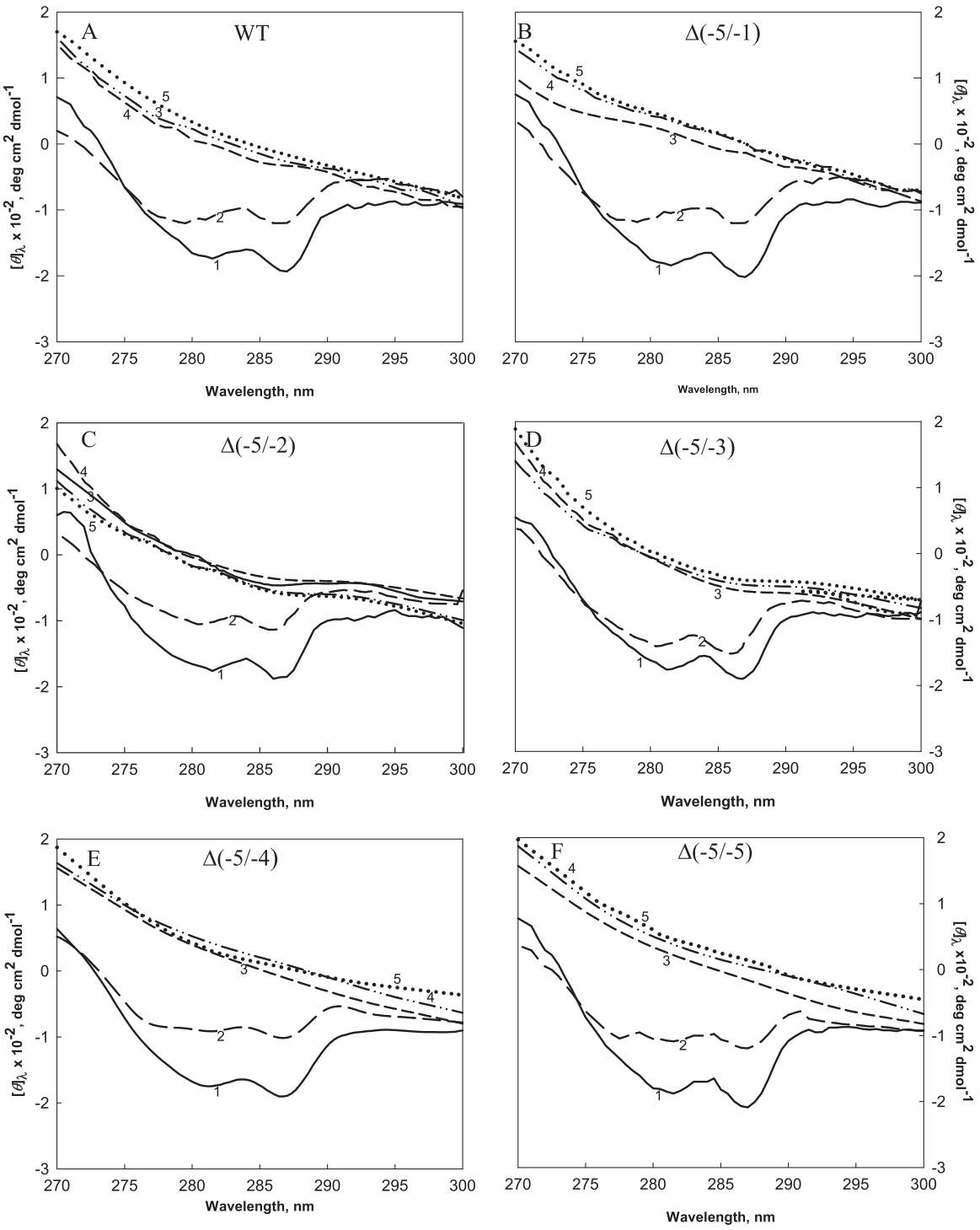

Fig. 5. The near-UV CD spectra of various states of WT y-cyt-*c* and its deletants at pH 6.0 and 25 °C. Native protein (curve 1); A state (curve 2); LiCl-induced X state (curve 3); LiCl-induced D state (curve 4); and urea-induced D state (curve 5). The curve numbers have the same meaning in all panels.

agreement with the one reported elsewhere [56]. The near-UV CD spectra of all deletants in the native state are, within experimental errors, comparable with that of the native WT protein as reported earlier [34]. Absence of dichroic bands in the near-UV region in urea/GdmCl denatured WT y-cyt-*c* (D state) has been attributed to the absence of tertiary interactions in the protein [56,57]. A comparison of the near-UV CD spectrum of the LiCl-induced X state (curve 3) and D state (curve 4) of the WT protein (Fig. 5A) with that of the urea-induced D state (curve 5) shows that the characteristic CD peaks are completely lost in the LiCl-induced X and D states, suggesting loss of tertiary structure in these states. Like X state of the WT protein, X state of all deletants has lost the characteristic bands in the near-UV region (Fig. 5B–F). Thus, examination of the near-UV CD suggests that X state observed during LiCl-induced denaturation at pH 6.0 and 25 °C fulfills another characteristic of PMG, namely, loss all the native tertiary structure [35,36].

To confirm further that X state of all proteins are indeed devoid of tertiary structure, we looked at the nature of the Met80–Fe

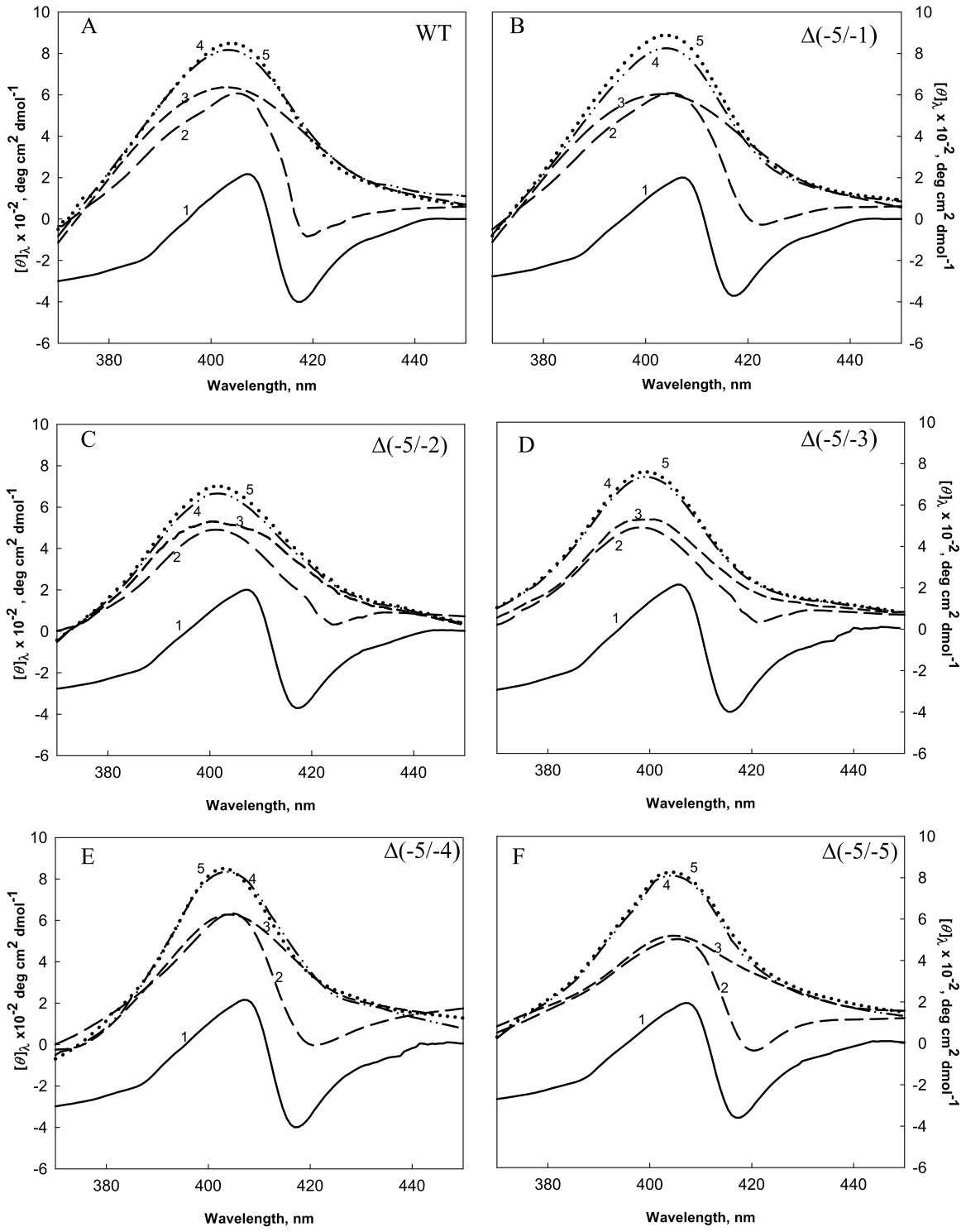

Fig. 6. Soret CD spectra of various states of WT y-cyt-*c* and its deletants at pH 6.0 and 25 °C. Native protein (curve 1); A state (curve 2); LiCl-induced X state (curve 3); LiCl-induced D state (curve 4); and urea-induced D state (curve 5). The curve numbers have the same meaning in all panels.

ligation in different states of the WT protein and its deletants. This interaction can be monitored by two independent probes, namely, CD band at 416 nm [58,59] and absorption band at 695 nm [47,60,61]. Fig. 6(A–F) shows the Soret CD spectra (450–370 nm) of the native protein (curve 1), LiCl-induced X state (curve 3) and denatured states induced by LiCl (curve 4) and urea (curve 5). The CD band at 416 nm is sensitive to the strength of heme-Met80 and Phe82-heme interaction [58,59]. It is seen in Fig. 6 that the native CD band at 416 nm is lost in X and D states of the protein. Disappearance of this band suggests disruption of Met80-heme coordination and disturbance in immediate environment of the heme [59,62,63]. Fig. 7(A–F) shows the absorption spectrum in the range 800–600 nm of the native proteins (curve 1), LiCl-induced X state (curve 3) and LiCl-induced D state (curve 4). It is seen in this figure that the 695 nm absorption band which is a signature of the presence of Met80–Fe interaction is lost in X and D states [60,61]. Thus, characterization of X state by the near-UV CD (Fig. 5), Soret CD (Fig. 6), and absorbance spectra (Fig. 7) led us to conclude

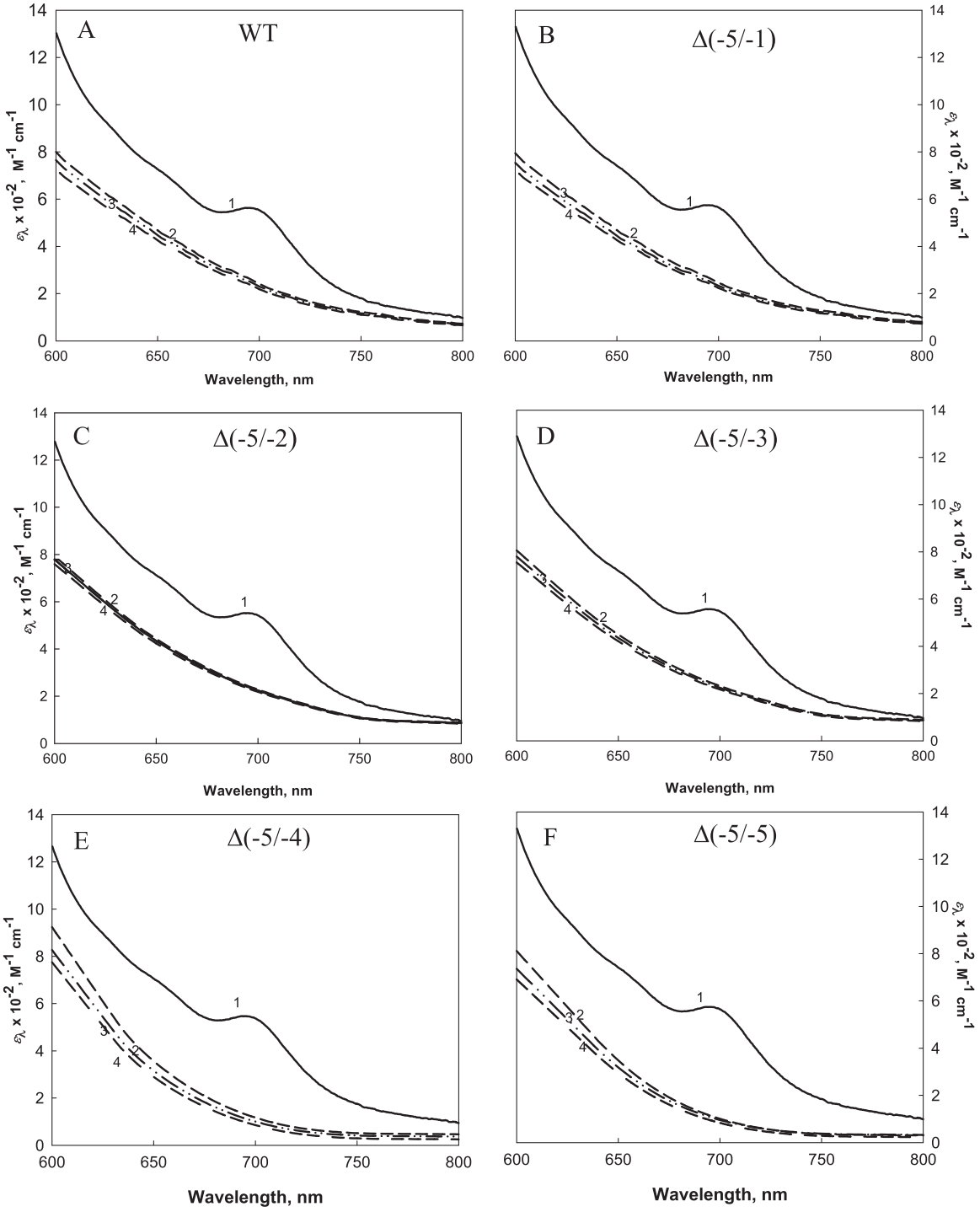

Fig. 7. Absorption spectra of WT y-cyt-*c* and its deletants at pH 6.0 and 25 °C. Native protein (curve 1); A state (curve 2); LiCl-induced X state (curve 3) and LiCl-induced D state (curve 4). The curve numbers have the same meaning in all panels.

that the intermediate state X is, indeed, devoid of tertiary interactions present in the native protein [27,28,36]. It is interesting to recall earlier studies [64–67] showing the disruption of the native Met-80-Fe ligation.

To provide further evidence that X state is PMG state, we carried out fluorescence measurements of ANS in the presence of WT protein and its deletants in the native state (curve1), X state (curve 3) and LiCl-induced D states (curve 4) at pH 6.0 and 25 °C (see Fig. 8). Fig. 8 also shows spectra of A state (curve 2) which will later be shown to have all characteristics of MG state. ANS in polar solvents has negligible emission spectrum. However, its binding with solvent exposed hydrophobic patches causes considerable increase in fluorescence intensity with a blue shift in its spectrum [68–70]. Generally, native state of a globular protein possess tightly packed, solvent inaccessible hydrophobic core that prevents ANS to bind to it. D state also does not bind ANS due to high polypeptide chain flexibility and complete loss of hydrophobic clusters [71]. It is seen in Fig. 8 that fluorescence spectra of ANS in the absence (curve 0) and presence of each protein in the native state (curve 1) and denatured state (curve 4) are indistinguishable, suggesting no ANS binding to N and D states of these proteins.

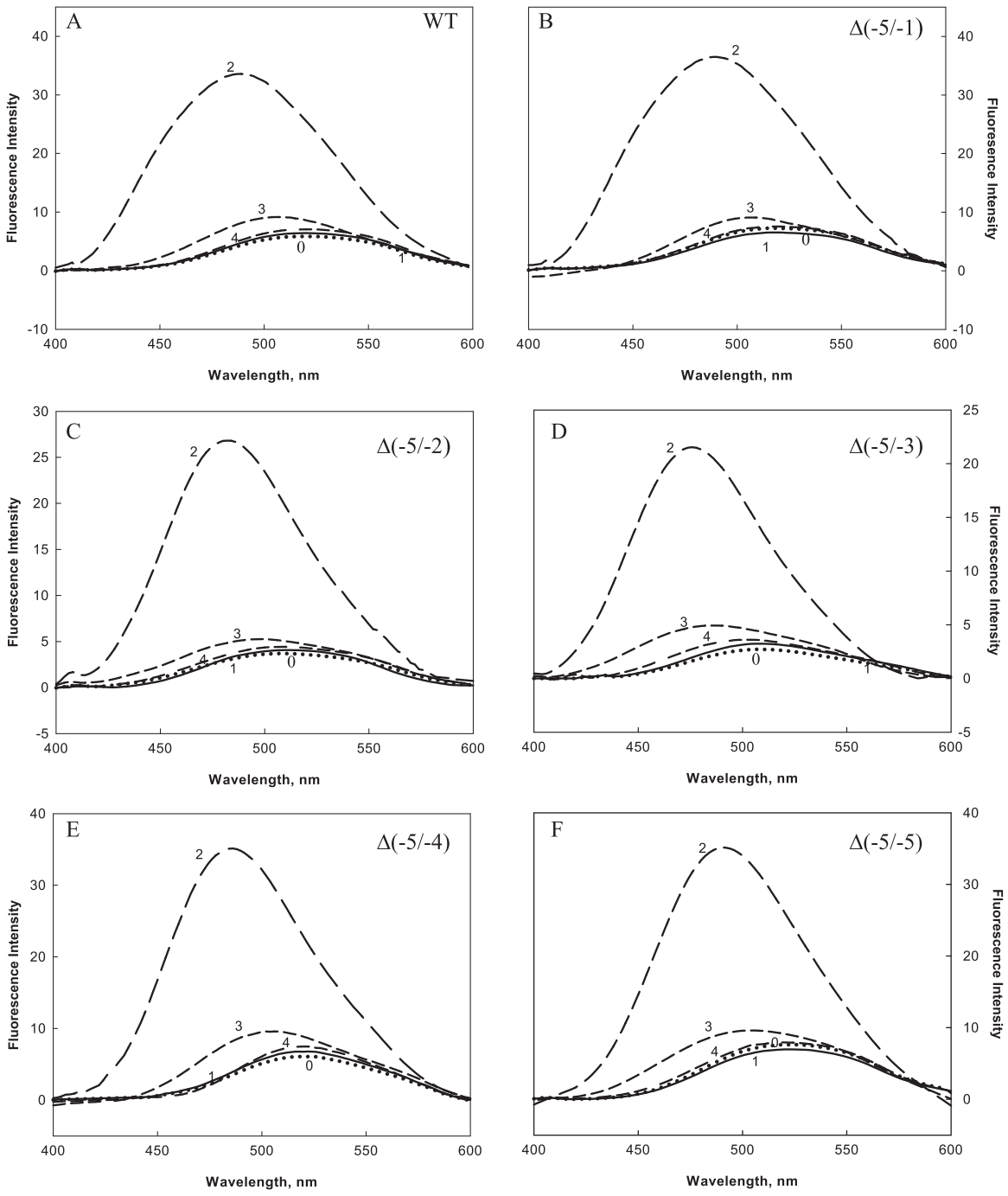

Fig. 8. ANS fluorescence spectra in the absence and presence of WT y-cyt-*c* and its deletants at pH 6.0 and 25 °C. Free ANS (curve 0), native state (curve 1), A-state (curve 2), LiCl-induced X state (curve 3), and LiCl-induced D state (curve 4). The curve numbers have the same meaning in all panels.

MG is an intermediate state between N and D states, which retains secondary structure and is compact enough to maintain solvent exposed hydrophobic clusters together, thus providing stronger affinity for ANS to bind [71–74]. PMG state that lies in between the MG state and the D state retains few hydrophobic patches [35,36,71,75]. It has been reported that ANS binding capacity of PMG state is approximately five times weaker in terms of fluorescence intensity than that of the MG state [35,36,71,75]. It is seen in Fig. 8 that there is a blue shift in spectra of both X and A states suggesting ANS binding in these states. Fig. 8 and Table 1 also show that fluorescence intensity of X state (curve 3) of each protein (WT and its deletants) is approximately five times less than the fluorescence intensity of its respective A state (curve 2). These measurements thus suggest that X state is PMG state, for it fulfills another criterion of PMG state, namely (d) mentioned above [35,36].

To further characterize LiCl-induced X state, we estimated hydrodynamic volumes of proteins from their observed hydrodynamic radii obtained from DLS measurements in various solvent conditions. It is evident from results given in Table 1 that the hydrodynamic volume of LiCl-induced X state of each protein is approximately three times more than that of its native state – a condition for PMG, i.e., the compactness (in terms of hydrodynamic volume) is approximately three times more than that of the native protein. It has also been reported that the hydrodynamic volume of the denatured state is 12 times more than that of the native

Table 1
Averaged thermodynamic parameters associated with LiCl-induced denaturation of WT and its deletants monitored by change in $[\theta]_{222}$, $\Delta[\theta]_{409}$ and $\Delta\varepsilon_{405}$ at pH 6.0 and 25 °C.

Protein	Transition	ΔG_I^0 or ΔG_{II}^X or ΔG_D^0 (kcal mol^{-1})	m_I or m_{II} (kcal mol^{-1} M^{-1})	C_{mI} or C_{mII} (M)
WT	N ↔ X	5.05 ± 0.38	1.25 ± 0.14	4.05 ± 0.30
	X ↔ D	1.80 ± 0.13	1.85 ± 0.13	6.37 ± 0.38
	N ↔ D	(6.04 ± 0.44)[a]		
Δ(−5/−5)	N ↔ X	4.17 ± 0.26	1.01 ± 0.04	4.14 ± 0.29
	X ↔ D	1.99 ± 0.19	2.03 ± 0.12	6.40 ± 0.24
	N ↔ D	(5.48 ± 0.32)		
Δ(−5/−4)	N ↔ X	5.36 ± 0.44	1.20 ± 0.04	4.43 ± 0.32
	X ↔ D	2.18 ± 0.21	2.42 ± 0.06	6.49 ± 0.26
	N ↔ D	(6.90 ± 0.36)		
Δ(−5/−3)	N ↔ X	4.24 ± 0.35	1.02 ± 0.07	4.06 ± 0.24
	X ↔ D	1.93 ± 0.14	1.98 ± 0.09	6.37 ± 0.36
	N ↔ D	(5.68 ± 0.23)		
Δ(−5/−2)	N ↔ X	4.14 ± 0.24	1.01 ± 0.09	3.99 ± 0.29
	X ↔ D	2.00 ± 0.19	2.01 ± 0.09	6.45 ± 0.36
	N ↔ D	(5.53 ± 0.27)		
Δ(−5/−1)	N ↔ X	4.27 ± 0.34	1.10 ± 0.11	3.90 ± 0.30
	X ↔ D	1.89 ± 0.21	1.91 ± 0.09	6.38 ± 0.37
	N ↔ D	(5.20 ± 0.35)		

[a] Values in parentheses represent ΔG_D^0 associated with N ↔ D transitions induced by urea at pH 6.0 and 25 °C (unpublished results)

protein [35,36]. It is interesting to note that the hydrodynamic volumes obtained for D states of WT y-cyt-*c* and its deletants are also 12 times more than that of their respective native states (Table 1).

All structural measurements of the LiCl-induced X state at pH 6.0 and 25 °C suggest that the X state shows all the common characteristics of the PMG state.

4.2. Molten globule state

A state of WT y-cyt-*c* has been shown to resemble MG state [42,43]. To confirm whether A state of N-terminal deletants of WT y-cyt-*c* also resembles MG state under identical solvent conditions, we carried out structural characterization of A state of all deletants. The characteristics of MG state are: (a) the presence of pronounced amount of secondary structure, (b) the absence of most of the specific tertiary structure produced by tight packing of side chains, (c) presence of loosely packed hydrophobic core that increases the hydrophobic surface accessible to the solvent, and (d) hydrodynamic volume is 1.5 times more than that of the native protein [35,36,75]. The far-UV CD spectra of A state of WT y-cyt-*c* and its deletants (curve 2, Fig. 4) show no change in the secondary structure content as compared to that present in the N state (curve 1) of respective proteins (see Table 1). It suggests absolute retention of the secondary structure, which is in accordance with the first criterion of MG state mentioned above. The near-UV CD spectra of A state of all proteins (curve 2, Fig. 5) show that the peaks, in the region 282–289 nm, characteristics of the native proteins (curve 1) are diminished. The spectrum of A state lies in between the spectra of completely folded (curve1) and unfolded (curves 3–5) proteins. The near-UV CD spectra of A state (curve 2, Fig. 5) of all proteins suggest partial loss of tertiary structure. Partial loss of CD band at 416 nm in the Soret CD spectrum (Fig. 6) and complete loss of absorption band at 695 nm (Fig. 7) in A state (curve 2) imply disruption of Met80–Fe interaction in all proteins. These near-UV and Soret CD and absorption measurements show partial perturbation in the tertiary structure of proteins, and fulfill the above mentioned second criterion, (b). ANS fluorescence of A state (Fig. 8) shows 5–7 fold increment in the intensity of ANS as compared to that of N state implying increased exposure of hydrophobic patches that binds to ANS. This observation fulfils another criterion of MG state, namely, criterion (c) mentioned above. Lastly, the hydrodynamic volume of A state determined by DLS measurements (Table 1) is approximately 1.5 times larger than that of the N state of respective proteins, fulfilling the last criterion of being a MG, namely, criterion (d) mentioned above [75]. Thus all pieces of structural evidence imply that A state of each deletant of WT y-cyt-*c* is a MG state as observed for other cyts-*c* [42,43,56,76–90].

Equilibrium denaturation curves induced by the weak salt denaturant, LiCl monitored by $\Delta\varepsilon_{405}$, $\Delta[\theta]_{409}$ and $[\theta]_{222}$, are biphasic (N ↔ X ↔ D) transitions (Figs. 1, 2 and S1–S4). This observation provides evidence that there exists a thermodynamically stable intermediate at pH 6.0 and 25 °C, which gets accumulated in a very narrow range of LiCl concentration. We analyzed the transitions N ↔ X (transition I) and X ↔ D (transition II) for thermodynamic parameters, ΔG, m and C_m of the WT protein and its deletants. The averaged values of these parameters, estimated from different optical probes are given in Table 2. It is important to note that for the analysis of these transitions, following assumptions were made. First, each transition (i.e., N ↔ X and X ↔ D) follows a two-state mechanism. A test of this assumption is to see whether one gets comparable thermodynamic parameters associated with the transition curves monitored by different structural probes. It is clear from Figs. 3, S5 and S6 that, for each transition, f and ΔG values from different optical probes fall on the same f versus [LiCl] and ΔG versus [LiCl] curves, respectively. This is taken as evidence for transitions N ↔ X and X ↔ D to be two-state processes [91]. A more reliable test for the authenticity of two-state assumption is to compare the total Gibbs free energy change of each protein associated with N ↔ X ↔ D observed here with that obtained for N ↔ D transition induced.

Values for ΔG_D^0 associated with two-state N ↔ D transition of the WT protein and its deletants are not reported in the literature. We have measured urea-induced denaturation curves of all proteins followed by monitoring changes in $[\theta]_{222}$, $[\theta]_{405}$ and $\Delta\varepsilon_{405}$ at pH 6.0 and 25 °C (unpublished results). It has been observed that the normalized denaturation curves of all these optical properties coincide with each other, suggesting that urea induces a two-state denaturation. Each denaturation curve was analyzed to determine values of ΔG_D^0 associated with N ↔ D transition, and the values are shown for comparison in Table 2. It is seen in this table that the sum of ΔG_I^0 and ΔG_{II}^X for each protein is, within experimental errors, identical to ΔG_D^0 associated with N ↔ D process.

Table 2
Comparison of the different structural properties of different states of y-cyt-*c* and its deletants at pH 6.0 and 25 °C.

Protein	State	Property		
		$[\theta]_{222}$ (deg cm^2 dmol^{-1})	ANS fluorescence at λ_{max}	Hydrodynamic volume (Å^3)
WT	N	−12,232 ± 187	6.7 ± 0.5	14,427 ± 577
	A	−11,969 ± 172	34.0 ± 1.9	23,633 ± 976
	X	−6738 ± 151	9.3 ± 1.1	41,646 ± 1190
	D	−2198 ± 158	7.1 ± 0.3	166,160 ± 4312
Δ(−5/−1)	N	−11,144 ± 182	6.5 ± 0.6	15,508 ± 623
	A	−10,761 ± 188	37.0 ± 2.0	24,438 ± 848
	X	−5657 ± 162	8.8 ± 1.3	39,927 ± 1253
	D	2136 ± 154	7.8 ± 0.4	163,253 ± 4415
Δ(−5/−2)	N	−10,882 ± 192	4.06 ± 0.5	13,573 ± 529
	A	−10,656 ± 169	26.8 ± 2.0	22,057 ± 908
	X	−5867 ± 142	5.2 ± 0.5	45,193 ± 1246
	D	−1875 ± 139	4.4 ± 0.6	156,006 ± 4284
Δ(−5/−3)	N	−10,908 ± 189	3.2 ± 0.4	13,299 ± 597
	A	−10,635 ± 171	21.5 ± 1.6	20,570 ± 734
	X	−5716 ± 153	4.9 ± 0.5	43,977 ± 1279
	D	−1961 ± 144	3.6 ± 0.5	163,118 ± 4402
Δ(−5/−4)	N	−11,244 ± 170	6.9 ± 0.5	13,588 ± 369
	A	−10,944 ± 162	35.0 ± 2.0	24,469 ± 774
	X	−5723 ± 155	9.6 ± 1.3	36,124 ± 1418
	D	−1878 ± 130	7.8 ± 0.5	145,191 ± 2680
Δ(−5/−5)	N	−11,689 ± 180	6.8 ± 0.5	16,227 ± 624
	A	−11,389 ± 135	34.9 ± 1.7	22,856 ± 783
	X	−6018 ± 160	9.6 ± 1.3	41,080 ± 1157
	D	−1986 ± 126	7.5 ± 0.5	167,652 ± 3963

Second, it was assumed that ΔG_{I} and ΔG_{II} vary linearly with LiCl concentration. It has been shown earlier [30] that the plot ΔG versus [LiCl] is linear in cases of horse and bovine cyts-*c*. We believe that it is also true in cases of proteins studied here.

In our earlier study, we have shown the effect of deletion of N-terminal extension on the thermodynamic stability of WT y-cyt-*c* [34]. The order of stability obtained from heat-induced denaturation of the WT protein and its deletants is: Δ(−5/−4) > WT > Δ(−5/−3) > Δ(−5/−5) > Δ(−5/−2) ∼ Δ(−5/−1). This order of stability has been explained using *in silico* analysis [34]. As evident from Table 2, the stability ($\Delta G = \Delta G_{\mathrm{I}}^{0} + \Delta G_{\mathrm{II}}^{\mathrm{X}}$) of all proteins associated with the LiCl-induced biphasic denaturation, N ↔ X ↔ D, follows the similar order as was observed for the heat-induced denaturation of these proteins. This observation suggests that deletion of N-terminal extension does affect the stability of the N state of WT protein. Furthermore, it also validates our previous conclusion that deletion contributes to the stability of N state [34].

It is also evident from the values of $\Delta G_{\mathrm{II}}^{\mathrm{X}}$ given in Table 2 that the stability of X state of each protein with respect to D state is, with in experimental errors, comparable with each other. This finding led us to conclude that deletion of extra N-terminal residues does not affect the stability of the pre-molten globule (X state) state in terms of Gibbs free energy change. On the basis of the results obtained in this study it is possible to conclude that (a) the thermodynamically stable intermediate state exists on the reversible folding/unfolding pathway of y-cyt-*c* and its deletants at pH 6.0 and 25 °C, (b) this folding intermediate has all the common characteristics of PMG state, and (c) the deletion of one or more of the extra five N-terminal residues has no effect on the stability of PMG state.

Acknowledgments

MAH, SU and SZ are thankful to University Grants Commission (Government of India), Department of Biotechnology (Government of India) and Indian Council of Medical Research (Government of India), respectively for their fellowships. FA and MIH gratefully acknowledge the financial support from the Department of Science and Technology, Ministry of Science and Technology (SB/SO/BB-71/2010(G)).

Appendix A. Supplementary data

Supplementary data associated with this article can be found, in the online version, at http://dx.doi.org/10.1016/j.ijbiomac.2014.10.053.

References

[1] C.B. Anfinsen, Science 181 (1973) 223–230.
[2] C. Levinthal, J. Chim. Phys. 65 (1968) 44.
[3] M. Tsytlonok, L.S. Itzhaki, Arch. Biochem. Biophys. 531 (2013) 14–23.
[4] O. Miyashita, J.N. Onuchic, P.G. Wolynes, Proc. Natl. Acad. Sci. U.S.A. 100 (2003) 12570–12575.
[5] C. Hyeon, P.A. Jennings, J.A. Adams, J.N. Onuchic, Proc. Natl. Acad. Sci. U.S.A. 106 (2009) 3023–3028.
[6] S.M. Truhlar, E. Mathes, C.F. Cervantes, G. Ghosh, E.A. Komives, J. Mol. Biol. 380 (2008) 67–82.
[7] K.L. Thoren, E.J. Worden, J.M. Yassif, B.A. Krantz, Proc. Natl. Acad. Sci. U.S.A. 106 (2009) 21555–21560.
[8] M.T. Honaker, M. Acchione, W. Zhang, B. Mannervik, W.M. Atkins, J. Biol. Chem. 288 (2013) 18599–18611.
[9] K. Pervushin, K. Vamvaca, B. Vogeli, D. Hilvert, Nat. Struct. Mol. Biol. 14 (2007) 1202–1206.
[10] T. Eichner, A.P. Kalverda, G.S. Thompson, S.W. Homans, S.E. Radford, Mol. Cell 41 (2011) 161–172.
[11] T.R. Jahn, M.J. Parker, S.W. Homans, S.E. Radford, Nat. Struct. Mol. Biol. 13 (2006) 195–201.
[12] R. Herbst, K. Gast, R. Seckler, Biochemistry 37 (1998) 6586–6597.
[13] L. Acosta-Sampson, J. King, J. Mol. Biol. 401 (2010) 134–152.
[14] S. Zaidi, M.I. Hassan, A. Islam, F. Ahmad, Cell. Mol. Life Sci. 71 (2014) 229–255.
[15] R.A. Goldbeck, E. Chen, D.S. Kliger, Int. J. Mol. Sci. 10 (2009) 1476–1499.
[16] A.P. Capaldi, C. Kleanthous, S.E. Radford, Nat. Struct. Biol. 9 (2002) 209–216.
[17] F.A. Tezcan, W.M. Findley, B.R. Crane, S.A. Ross, J.G. Lyubovitsky, H.B. Gray, J.R. Winkler, Proc. Natl. Acad. Sci. U.S.A. 99 (2002) 8626–8630.
[18] R. Grandori, Protein Sci. 11 (2002) 453–458.
[19] S.R. Yeh, D.L. Rousseau, Nat. Struct. Biol. 5 (1998) 222–228.
[20] H. Roder, G.A. Elove, S.W. Englander, Nature 335 (1988) 700–704.
[21] T.R. Sosnick, L. Mayne, R. Hiller, S.W. Englander, Nat. Struct. Biol. 1 (1994) 149–156.
[22] W. Colon, G.A. Elove, L.P. Wakem, F. Sherman, H. Roder, Biochemistry 35 (1996) 5538–5549.

[23] S. Akiyama, S. Takahashi, K. Ishimori, I. Morishima, Nat. Struct. Biol. 7 (2000) 514–520.
[24] A.F. Chaffotte, Y. Guillou, M.E. Goldberg, Biochemistry 31 (1992) 9694–9702.
[25] O.B. Ptitsyn, Adv. Protein Chem. 47 (1995) 83–229.
[26] A.L. Fink, L.J. Calciano, Y. Goto, T. Kurotsu, D.R. Palleros, Biochemistry 33 (1994) 12504–12511.
[27] V.N. Uversky, O.B. Ptitsyn, Biochemistry 33 (1994) 2782–2791.
[28] V.N. Uversky, O.B. Ptitsyn, J. Mol. Biol. 255 (1996) 215–228.
[29] B. Moza, S.H. Qureshi, A. Islam, R. Singh, F. Anjum, A.A. Moosavi-Movahedi, F. Ahmad, Biochemistry 45 (2006) 4695–4702.
[30] S.H. Qureshi, B. Moza, S. Yadav, F. Ahmad, Biochemistry 42 (2003) 1684–1695.
[31] M.K. Alam Khan, M.H. Rahaman, M.I. Hassan, T.P. Singh, A.A. Moosavi-Movahedi, F. Ahmad, J. Biol. Inorg. Chem. 15 (2010) 1319–1329.
[32] M.K. Alam Khan, U. Das, M.H. Rahaman, M.I. Hassan, A. Srinivasan, T.P. Singh, F. Ahmad, J. Biol. Inorg. Chem. 14 (2009) 751–760.
[33] G.R. Moore, G.W. Pettigrew, Cytochrome c: Evolutionary, structural and physicochemical aspects, Springer-Verlag, Berlin, 1990, pp. 831–833.
[34] S. Ubaid-Ullah, M.A. Haque, S. Zaidi, M.I. Hassan, A. Islam, J.K. Batra, T.P. Singh, F. Ahmad, J. Biomol. Struct. Dyn. 32 (2014) 2005–2016.
[35] V.N. Uversky, Protein Pept. Lett. 4 (1997) 355–367.
[36] V.N. Uversky, Protein Sci. 11 (2002) 739–756.
[37] C.M. Lett, M.D. Rosu-Myles, H.E. Frey, J.G. Guillemette, Biochim. Biophys. Acta 1432 (1999) 40–48.
[38] D.S. Cohen, G.J. Pielak, Protein Sci. 3 (1994) 1253–1260.
[39] R.L. Cutler, G.J. Pielak, A.G. Mauk, M. Smith, Protein Eng. 1 (1987) 95–99.
[40] Y. Goto, N. Takahashi, A.L. Fink, Biochemistry 29 (1990) 3480–3488.
[41] E. Margoliash, N. Frohwirt, Biochem J. 71 (1959) 570–572.
[42] J.L. Marmorino, M. Lehti, G.J. Pielak, J. Mol. Biol. 275 (1998) 379–388.
[43] J.L. Marmorino, G.J. Pielak, Biochemistry 34 (1995) 3140–3143.
[44] P.M. Mulqueen, M.J. Kronman, Arch. Biochem. Biophys. 215 (1982) 28–39.
[45] R.C. Weast, Handbook of Chemistry and Physics, 53rd ed., CRC Press, Cleveland, OH, 1972.
[46] A. Schejter, W.A. Eaton, Biochemistry 23 (1984) 1081–1084.
[47] E. Margoliash, A. Schejter, Adv. Protein Chem. 21 (1966) 113–286.
[48] C.N. Pace, CRC Crit. Rev. Biochem. 3 (1975) 1–43.
[49] G. Blauer, N. Sreerama, R.W. Woody, Biochemistry 32 (1993) 6674–6679.
[50] Y.P. Myer, J. Biol. Chem. 243 (1968) 2115–2122.
[51] Y.P. Myer, Methods Enzymol. 54 (1978) 249–284.
[52] N. Greenfield, G.D. Fasman, Biochemistry 8 (1969) 4108–4116.
[53] N.J. Greenfield, Nat. Protoc. 1 (2006) 2876–2890.
[54] L.M. Herrmann, B.E. Bowler, Protein Sci. 6 (1997) 657–665.
[55] A.M. Davies, J.G. Guillemette, M. Smith, C. Greenwood, A.G. Thurgood, A.G. Mauk, G.R. Moore, Biochemistry 32 (1993) 5431–5435.
[56] F. Sinibaldi, B.D. Howes, M.C. Piro, P. Caroppi, G. Mei, F. Ascoli, G. Smulevich, R. Santucci, J. Biol. Inorg. Chem. 11 (2006) 52–62.
[57] Y.P. Myer, L.H. MacDonald, B.C. Verma, A. Pande, Biochemistry 19 (1980) 199–207.
[58] G.J. Pielak, K. Oikawa, A.G. Mauk, M. Smith, C.M. Kay, J. Am. Chem. Soc. 108 (1986) 2724–2727.
[59] R. Santucci, F. Ascoli, J. Inorg. Biochem. 68 (1997) 211–214.
[60] A. Schejter, P. George, Biochemistry 3 (1964) 1045–1049.
[61] E. Stellwagen, R. Cass, Biochem. Biophys. Res. Commun. 60 (1974) 371–375.
[62] M.C. Hsu, R.W. Woody, J. Am. Chem. Soc. 93 (1971) 3515–3525.
[63] Y.P. Myer, H.A. Harbury, J. Biol. Chem. 241 (1966) 4299–4303.
[64] W. Colon, L.P. Wakem, F. Sherman, H. Roder, Biochemistry 36 (1997) 12535–12541.
[65] K. Muthukrishnan, B.T. Nall, Biochemistry 30 (1991) 4706–4710.
[66] J. Babul, E. Stellwagen, Biochemistry 11 (1972) 1195–1200.
[67] E. Chen, C.J. Abel, R.A. Goldbeck, D.S. Kliger, Biochemistry 46 (2007) 12463–12472.
[68] O.B. Ptitsyn, Curr. Opin. Struct. Biol. 5 (1995) 74–78.
[69] O.B. Ptitsyn, Trends Biochem. Sci. 20 (1995) 376–379.
[70] O.B. Ptitsyn, R.H. Pain, G.V. Semisotnov, E. Zerovnik, O.I. Razgulyaev, FEBS Lett. 262 (1990) 20–24.
[71] G.V. Semisotnov, N.A. Rodionova, O.I. Razgulyaev, V.N. Uversky, A.F. Gripas, R.I. Gilmanshin, Biopolymers 31 (1991) 119–128.
[72] D.A. Dolgikh, L.V. Abaturov, I.A. Bolotina, E.V. Brazhnikov, V.E. Bychkova, R.I. Gilmanshin, O. Lebedev Yu, G.V. Semisotnov, E.I. Tiktopulo, O.B. Ptitsyn, et al., Eur. Biophys. J. 13 (1985) 109–121.
[73] K.P. Wong, L.M. Hamlin, Biochemistry 13 (1974) 2678–2683.
[74] K.P. Wong, C. Tanford, J. Biol. Chem. 248 (1973) 8518–8523.
[75] M. Arai, K. Kuwajima, Adv. Protein Chem. 53 (2000) 209–282.
[76] T.V. Chalikian, V.S. Gindikin, K.J. Breslauer, J. Mol. Biol. 250 (1995) 291–306.
[77] W. Colon, H. Roder, Nat. Struct. Biol. 3 (1996) 1019–1025.
[78] Y. Goto, L.J. Calciano, A.L. Fink, Proc. Natl. Acad. Sci. U.S.A. 87 (1990) 573–577.
[79] Y. Goto, Y. Hagihara, D. Hamada, M. Hoshino, I. Nishii, Biochemistry 32 (1993) 11878–11885.
[80] Y. Hagihara, Y. Tan, Y. Goto, J. Mol. Biol. 237 (1994) 336–348.
[81] M.F. Jeng, S.W. Englander, G.A. Elove, A.J. Wand, H. Roder, Biochemistry 29 (1990) 10433–10437.
[82] M. Kataoka, Y. Hagihara, K. Mihara, Y. Goto, J. Mol. Biol. 229 (1993) 591–596.
[83] T. Konno, Protein Sci. 7 (1998) 975–982.
[84] Y. Kuroda, S. Endo, K. Nagayama, A. Wada, J. Mol. Biol. 247 (1995) 682–688.
[85] S. Nakamura, Y. Seki, E. Katoh, S. Kidokoro, Biochemistry 50 (2011) 3116–3126.
[86] R. Santucci, C. Bongiovanni, G. Mei, T. Ferri, F. Polizio, A. Desideri, Biochemistry 39 (2000) 12632–12638.
[87] F. Sinibaldi, B.D. Howes, G. Smulevich, C. Ciaccio, M. Coletta, R. Santucci, J. Biol. Inorg. Chem. 8 (2003) 663–670.
[88] F. Sinibaldi, M.C. Piro, M. Coletta, R. Santucci, FEBS J. 273 (2006) 5347–5357.
[89] K.S. Vassilenko, V.N. Uversky, Biochim. Biophys. Acta 1594 (2002) 168–177.
[90] Q. Xu, T.A. Keiderling, Biopolymers 73 (2004) 716–726.
[91] K.A. Dill, Biochemistry 29 (1990) 7133–7155.